STABILITY AND TRANSITION IN CONTINUOUSLY DEFORMED CELLULAR AUTOMATA

ESTABILIDAD Y TRANSICIÓN EN AUTÓMATAS CELULARES CONTÍNUAMENTE DEFORMADOS

K. García-Medina[a], D. Estevez-Moya[a] y Ernesto Estevez-Rams [a,b†]

a) Facultad de Física, Universidad de la Habana, San Lázaro y L., 10400, La Habana, Cuba
b) Instituto de Ciencias y Tecnología de Materiales, University of Havana (IMRE); estevez@fisica.uh.cu
† corresponding author

The behavior of continuously deformed cellular automata rules is explored. The analysis is performed in terms of three entropic measures, entropy density, excess entropy, and entropy distance. These measures have been suggested to be indicative of the capabilities in the storage, processing, and transmission of information. A wealth of different behaviors is found that points to a richness of unexplored rules. Transitions can involve the loss of memory between the discrete rules at the start and end of the deformation parameter values. The behavior of the entropic measures, especially the surge of excess entropy on the verge of transition to disordered states, suggests the occurrence of enhanced computation at the edge of chaos for different types of phase transitions.

Se estudia el comportamiento de autómatas celulares contínuamente deformados. El análisis se efectúa en términos de magnitudes entrópicas indicativas de las capacidades del sistema de almacenar, producir y transportar información. Se hallíron una amplitud de comportamientos al abrir el espacio de reglas a un conjunto infinito irracional aún sin explorar. Transiciones pueden comprender la pérdida de memoria al comienzo y al final de la transición. Aumento de la capacidad de cómputo al borde del caos es hallado y se muestra que tal proceso puede ocurrir en diferentes tipos de transiciones de fases pero en todos los casos, caracterizada por un aumento brusco del exceso de entropía.

I. INTRODUCTION

The idea of a dynamical system as a computational system that stores, transmit, and produces information is a compelling one that has been the focus of attention for a while [1]. Cellular automata (CA) are a kind of system that can exhibit from very trivial behavior to very complex one, including universal Turing machine capabilities [2]. This richness of behavior comes despite being defined by local rules that act over a neighborhood for each given cell. The spatiotemporal diagrams of CA can show from complete randomness to long-range correlation both in the spatial and temporal dimensions (See [3] and reference therein).

The enhanced computation at the edge of chaos hypothesis (EOC) states that in certain dynamical systems, as the dynamics evolve towards a chaotic regime, improved computational capabilities of the system are claimed to be found on the verge of the transition [4–6]. Improved computational capabilities can mean that the system, given appropriate initial conditions, can perform some "useful" task. However, in a more general context, it can be taken to mean that the system is capable of improved capacity to store, transmit, and produce information in Shannon sense [7].

There are several natural and artificial systems where EOC has been claimed to occur [8–12]; CA has been one of them. Langton [5] used a *lambda* parameter, defined as the fraction of quiescent state in a CA rule. A quiescent state is an arbitrary chosen one. Langton [5] and afterward, Packard [13] performed numerical simulations to conclude

that, on average, as λ, increases from 0, the CA rules define spatiotemporal maps that change from a fixed point regime, to periodic, to complex and finally to chaotic behavior. Packard [13] even claimed that CA capable of algorithmic abilities were to be sought at those critical values of λ where a transition to the chaotic behavior occurs. Crutchfield et al. [7] performed extensive Monte Carlo simulations and failed to found EOC in the sense of Packard claim.

Recently Estevez et al. [14] have shown evidence of EOC in CA but in the broader sense and working with rules that can change continuously as a transition is made from one rule to another. The idea is to change one or several entries in the CA rule allowing a geometry to be introduced in the CA space. Two instances of EOC were reported by Estevez et al. as measured using entropic magnitudes that characterize spatial disorder or spatial structuring. The price paid for such continuous deformation of CA rules is that discrete states are abandoned. In their study, the λ parameter plays no role in the transition.

In this contribution, we further explore EOC in elementary CA. We introduce stability diagrams to characterize the robustness of rules under entries deformation. A classification of rule transition is attempted based on the observed experimental results. Several EOCs are reported and discussed in the text. The paper is organized as follows: first, CA are formally introduced, and continuous deformation of CA rules is defined following the pioneer works of Pedersen [15]. The entropic magnitudes used to characterize the dynamical behavior of the system are introduced. Results

are described from numerical simulations and discussed. Conclusion follows.

II. CELLULAR AUTOMATA

For the purpose of this paper a discrete cellular automaton can be defined by the tern (Σ, s, Φ), where Σ is a finite alphabet which will be taken as binary ($\Sigma = \{0, 1\}$); $s = s_0, s_1, \ldots s_{N-1}$ is a set of sites arranged in a ring, and; Φ is a local updating rule. If $s^t = s_0^t, s_1^t, \ldots s_{N-1}^t$ denotes a particular configuration of the sites values at time t, then

$$s_i^t = \Phi\left[s_{i-r}^{(t-1)}, \ldots, s_{i-1}^{(t-1)}, s_i^{(t-1)}, s_{i+1}^{(t-1)}, \ldots, s_{i+r}^{(t-1)}\right]. \quad (1)$$

We will be considering the so called elementary rules (ECA) where $r = 1$ and equation (1) reduces to

$$s_i^t = \Phi\left[s_{i-1}^{(t-1)}, s_i^{(t-1)}, s_{i+1}^{(t-1)}\right]. \quad (2)$$

The above definition leads to a look up table for the ECA rule,

s_{i-1}	s_i	s_{i+1}	rule
0	0	0	$\Phi(0,0,0)$
0	0	1	$\Phi(0,0,1)$
0	1	0	$\Phi(0,1,0)$
0	1	1	$\Phi(0,1,1)$
1	0	0	$\Phi(1,0,0)$
1	0	1	$\Phi(1,0,1)$
1	1	0	$\Phi(1,1,0)$
1	1	1	$\Phi(1,1,1)$

There are a total of $2^{2^3} = 256$ possible ECA rules which can be labelled in different ways. Wolfram numbering scheme assign to each rule Φ a label R according to [16]:

$$R = \Phi(0,0,0)2^0 + \Phi(0,0,1)2^1 + \Phi(0,1,0)2^2 + \ldots + \Phi(1,1,1)2^7. \quad (3)$$

Instead we can use the binary number $\Phi(1,1,1) \ldots \Phi(0,1,0) \Phi(0,0,1)\Phi(0,0,0)$, which is the binary representation of R. For example

$$01110110 \rightarrow R = 118$$

There are a total of $2^{2^3} = 256$ possible ECA rules.

Langston λ [5] parameter can be defined as

$$\lambda = \frac{[\Phi(1,1,1) + \ldots + \Phi(0,1,0) + \Phi(0,0,1) + \Phi(0,0,0)]}{8}$$

which is just the fraction of entries in the CA rule that turns a state into 1, taken as the quiescent state.

II.1. Continuous state CA

The ECA rules define a hypercube; each corner of the hypercube is labeled by a rule, so there are 256 corners. Two corners of the hypercube share and edge if they differ in only one entry. The construction is equivalent to a graph, each node of the graph represents a rule, and two nodes are linked by an edge if they differ in one entry. Figure 1 shows the local topology of the graph around one rule up to second neighbors. The problem of the discrete CA space is that two rules sharing an edge need not have a more similar behavior than two nodes that do not share an edge. There is no apparent geometry in the CA discrete space: In the ECA rules, no apparent geometric order can be defined, were behavior changes gradually as the system changes from one rule to the next in the ordering.
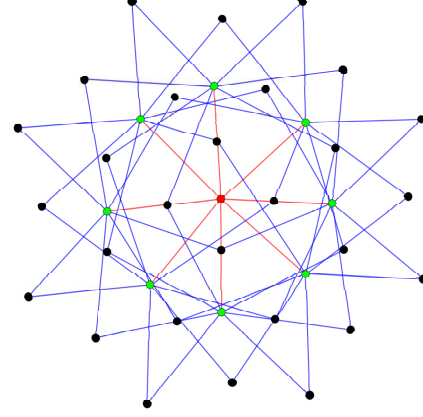

Figure 1. Local topology of the connectivity graph representing the ECA rules. Green nodes connected by red edges are the first neighbors. Black nodes represent the second neighbors. The complete graph of the 256 rules can be built around a central one by incorporating more coordination spheres.

In an attempt to define a gradual transition from one rule to another, Pedersen sacrificed the discrete nature of the CA rules and allowed to deform CA rules in a continuous way [15]. The idea goes as follows, Consider a rule with binary representation 01110110 (ECA: 118) and make any of the entries a continuous variable, for example, 01ξ10110, now ξ can change continuously from 1 to 0 and the initial binary rule changes gradually to the final binary rule 0101001 (ECA: 86) (See figure 2).

Figure 2. The transition from one rule to another as we continuously change an entry in the look-up table.

One can chose how when changing ξ the rule transforms, in a number of ways, whose specifics have been shown not to be essential for the analysis. We follow Pedersen [15]. A real valued function β, taken as $\beta(s_{i-1}s_is_{i+1}) = 4s_{i-1} + 2s_i + s_{i+1}$, and an interpolating function $f(x)$: $f(\beta(s_{i-1}s_is_{i+1})) : [0,7] \rightarrow [0,1]$ are defined. β will transform the neighborhood configuration into a real value which will be used as the argument of $f(x)$. On the other ahnd, the interpolating function must give the discrete case for integer values of its argument but, apart from that, can be chosen freely. Following Pedersen, a quadratic interpolating function will be used for non integer value of the argument x,

$$f(x) = \begin{cases} 2[f(n+1) - f(n)](x-n)^2 + f(n), & \text{for} \ \ n \le x \le n+1/2 \\ \\ 2[f(n) - f(n+1)](x-n-1)^2 + f(n+1), & \text{for} \ \ n+1/2 \le x \le n+1 \end{cases}, \tag{4}$$

while the corresponding discrete rule is used if the argument x is an integer. $n(\equiv \lfloor x \rfloor)$ is the largest integer smaller than x ($f(n)$ will therefore correspond to the discrete rule of the CA, already defined by Φ).

The introduction of a real variable ξ within a rule means that the states of the cells are no longer binary values $\{0, 1\}$ but any real value in the interval $[0, 1]$. In order to recover the binary values for the cell states, once all cell values have been updated, a threshold is calculated. All cell values above the threshold are taken as 1, 0 otherwise. As a threshold, the mean value over all cells at a given time is used. This discretization is again, the one followed by Pedersen, another choice would be to use the median as a threshold value. The later preserves the balance between the two states and removes any dynamic associated with the production of symbols.

The simulations were performed over a ring of 5×10^3 cells. As the initial configuration, random values were used (random binary digits were taken from www.random.org). The system was left to evolve for 5×10^3 time steps. Averaging over different initial conditions was done before presenting the results. It was noticed that the average result did not differ from the individual runs. We settle to present the average over ten different initial conditions, as increasing the number did not change the results. The last ten spatial configurations were taken for each run, so the final averaging was over 10^2 spatial configurations. Also, calculations were occasionally performed for 10^4, 5×10^4, 10^5, and 10^6 cells to see if size dependence was an issue in the simulations. In all cases, the result did not change with the number of cells.

A dynamical system is chaotic if and only if it is transitive, and its periodic points set is dense in the phase space [17]. For a system to be transitive, surjectivity is a necessary condition. Hedlund [18] has proved that a one-dimensional discrete CA is surjective if and only if is $k-$balanced for all $k \in \mathbb{N}$. In the case of ECA rules, a $1-$balance implies that the binary look-up table of the rule must have the same number of $0's$ and $1's$. We will consider a discrete binary CA $k-$balanced if, evolving from a random starting sequence, the fraction of one symbol (0 or 1) remains $1/2$ in the kth time step.

III. ENTROPIC MEASURES

Consider a bi-infinite sequence $S^{(t)} = \ldots s_{-2}^{(t)} s_{-1}^{(t)} s_0^{(t)} s_1^{(t)} s_2^{(t)} \ldots$, where $s_i^{(t)}$ is the binary symbol observed in the cell i at time step t. We denote by $S^{(t)}(i, L)$ the substring of length L, starting at cell s_i, and by $S(., L)$ the sequence of the substring regardless of the starting cell position $S(., L) = S(i, L)$. $p[S(., L)]$ is the probability of finding the sequence $S(., L)$ in the bi-infinite string. Shannon

block entropy of length L is given by,

$$H_S(L) = - \sum_{S(.,L)} p[S(., L)] \log p[S(., L)]. \tag{5}$$

where the sum goes over all possible sequences $S(., L)$ of length L. Entropy density can be written in terms of the block entropy,

$$h_\mu(S) = \lim_{L \to \infty} \frac{H_S(L)}{L}. \tag{6}$$

Shannon entropy density h_μ will be used as a measure of information production [19].

There are different procedures to estimate h_μ directly from the data [20, 21]. In this work, estimation via Lempel-Ziv factorization [22] will be used; details can be found elsewhere [23]. Our data for each estimation will be the 10^5 binary values of each configuration $s^{(}t)$ studied.

For a measure of the amount of structuring in a sequence, excess entropy E, originally termed as effective complexity measure [24], will be used. Let $I[X : Y] = H[X] + H[Y] - H[X, Y]$ be the mutual information between X and Y [19]. $I[X : Y]$ is a measure of the amount of information one variable carries regarding the other. Excess entropy measures the mutual information between two infinite halves of the sequence [24, 25],

$$E(S) \quad = I[\ldots, s_{-1} : s_0, s_1, \ldots], \tag{7}$$

that is, how much information one halve carries about the other and vice-versa. E measures the correlation at all scales in a process and is related to the intrinsic memory of a system, related to pattern production and context preservation [25]. Excess entropy is also estimated through Lempel-Ziv factorization using a random shuffle procedure [26], as explained in [14].

Finally, we need a measure of the sensitivity of the system evolution to the initial conditions. A fingerprint of chaoticity is that small perturbations of initial conditions lead to an exponential growth of the difference in the trajectories. We need a metric to measure a "distance"between two sequences, a trivial choice is the so called Hamming distance, which is the fraction of sites where both sequences are different [19]. The Hamming distance can be unsatisfactory for several reasons, consider, for example, a CA rule that merely shifts the initial string by one cell to the left. Hamming distance between two consecutive sequences could have maximum Hamming distance, and yet, the production of the new sequence is quite trivial. In contrast, we need a metric that captures the difficulty of predicting a second sequence from the knowledge of the first one. This type of distance is called information distance and will be denoted by $d(s, p)$. An information distance based

on algorithmic randomness [27] will be used. The algorithmic randomness (also known as Kolmogorov complexity) of a string $K(s)$ is the length of the shortest algorithm s^* capable of producing the string s on a Universal Turing Machine ($K(s) = |s^*|$). Accordingly, $K(s|p^*)$, known as algorithmic conditional randomness, is the length of the shortest program able to reproduce s if the program p^*, reproducing the string p, is given. $d(s, p)$ can be defined as [28],

$$d(s, p) = \frac{max\{K(s|p^*), K(p|s^*)\}}{max\{K(s), K(p)\}}. \tag{8}$$

$d(s, p)$ measures how "hard"is, from an algorithmic perspective, to reproduce string s and p: two sequences which can be derived one from the other by a small-sized algorithm, will result in a small $d(s, p)$. $d(s, p)$ will be estimated again using Lempel-Ziv factorization as explained in [23],

$$d_{LZ}(s, p) = \frac{h_\mu(sp) - min\{h_\mu(s), h_\mu(p)\}}{max\{h_\mu(s), h_\mu(p)\}}. \tag{9}$$

To test for chaoticity, d_{LZ} will be used in the following way, two identical initial conditions, only differing in one site s_i taken randomly, are left to evolve. After a sufficient number of time steps, the information distance between both systems is calculated using (9). In this way, d_{LZ} is a measure of the system sensitivity to a minimum perturbation of the initial state. We tested the results for different initial conditions, again no change was observed for averaging using more than ten pairs of initial conditions; the final averaging was therefore taken for 20 different pairs of initial conditions.

For a sequence, S, large values of excess entropy, and low values of entropy density signal the prevalence of patterns in the sequence and the lack of randomness or unpredictability. In such a case, observing a sufficiently long but finite substring of the sequence leads to a prediction of the whole string with a small error. It is said that the system has a large intrinsic memory, but a small information production, when the entropy density is high, and the excess entropy is low, predictability is hard and, regardless of the length of the observed substring, the reconstruction of the whole sequence can not be done with a small error [25]. It is said that the system has a high information production but small intrinsic memory.

In a random sequence, there are no correlations between cell values for any block length. For that reason, the mutual information between the sequence two halves is zero, and excess entropy is zero, the system has no intrinsic memory. Every cell value carries new information, as it can not be predicted from the knowledge of other cells, information production is high, and entropy density is near 1. A significant computational capability will need a balance between information production and information storage if we think of the computational capabilities as the system's ability to store, transmit, and modify information.

IV. RESULTS AND DISCUSSION

As already described, we perform a transformation between two discrete rules by changing one entry ξ in the rule table.

There is a new rule for each different real value of ξ; therefore, formally, an infinite number of rules can be found between the two discrete rules at the extreme. However, when analyzing entropy density and excess entropy of the "intermediate" rules, we find that there are intervals where the dynamic behavior of the rules do not change. At a certain value of the ξ parameter, a jump in h_μ and E is found. The jumps are taken as indicative of a "phase transition". In the whole range, $[0, 1]$ of variation of the ξ parameter, several of such jumps can occur. In our study we identified six different types of behaviors as a discrete ECA rule changes to another discrete ECA rule

1. There are no jumps in h_μ and E jumps in the whole region of variation of ξ. This can only happen if discrete ECA rules at both sides have the same type of spatiotemporal map.

2. There is a single jump in h_μ and E in the whole region of variation of ξ.

3. There are two jumps in h_μ and E in the whole region of variation of ξ. Usually, the first jump results in a high value of entropy density and a low value of excess entropy, the second jump is in the opposite.

4. h_μ and E shows irregular behavior with multiple jumps in the region of variation of ξ.

5. When transitioning to a high entropy density state, excess entropy shows a well-defined peak, which can be narrower or broader.

Some rules can show a mixture of behaviors.

Transition $238 \rightarrow 239$ is an example of the first type (Figure 3). Both discrete rules have trivial spatiotemporal maps: After a transient, they reduce any initial random condition to a sequence of $0's$.
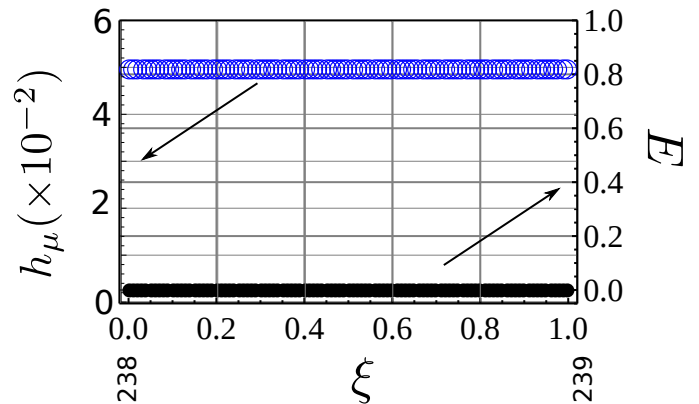

Figure 3. Entropy density (blue) and excess entropy (black) behaviour along the transition $238 \rightarrow 239$. Both end rules are trivial as they transform any initial condition to zero. The small value of h_μ above zero is consequence of the bias in the numerical estimation due to the finite nature of data. This is an example of type 1 transition.

For the other types of transitions, some jump in the entropic measures is found while changing the corresponding look-up table entry. It will be convenient to define a stability criteria that characterize how robust is a transition to changes in the ξ entry.

A stability parameter is defined for a given entry in a CA rule, as the value of ξ (ξ is changing from $0 \to 1$) or $1 - \xi$ (ξ is changing from $1 \to 0$) where a jump in the dynamical behavior is observed as measured by both h_μ and E. For each discrete state CA rule, we have a total of 8 possible transitions by changing each entry on the look-up table (figure 1).
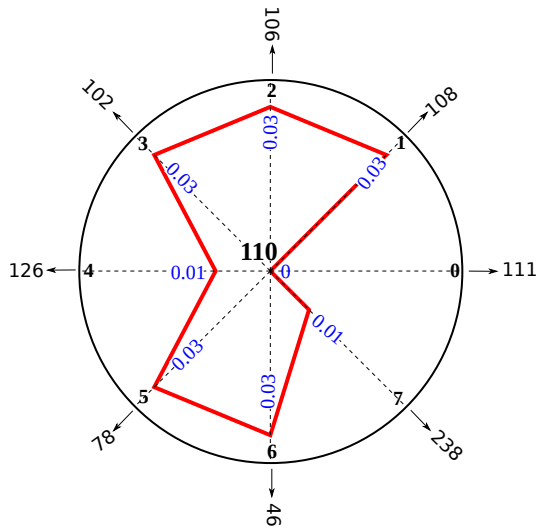

Figure 4. Stability diagram for rule 110. Changing each of the 8 entries in the look-up table determines a transition between ECA 110 and another ECA rule. In blue the stability value where a "phase" transition is seen as a jump in h_μ and E.
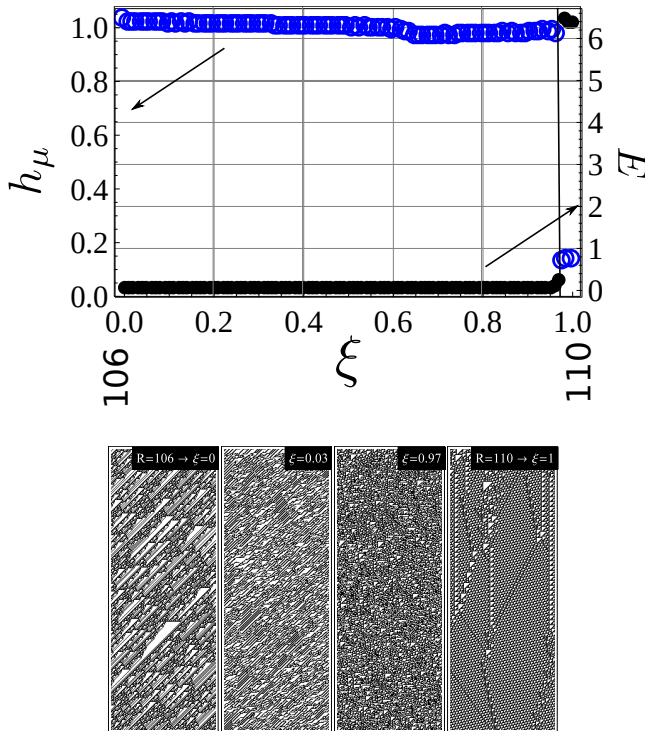

Figure 5. (up) Entropy density (blue) and excess entropy (black) behaviour along the transition 110(01101110) → 106(01101010). This type of transition is characterize by a single jump in the entropy density and the excess entropy in the whole range of the (01101ξ10) entry. Rule 110 is confirmed to be a complex rule capable of exhibiting universal Turing machine capabilities. (down) Spatio-temporal map the both discrete rules and two rules at intermediate values of ξ.

In figure 4 the stability diagram of rule 110 is shown. From the stability values, it is seen that rule 110 has a phase change

for rather small values: the rule is sensitive to small variations of its look-up table. Figure 5 (up) shows the change in the entropic measures as a function of ξ. For the transformation, 110 → 106, which corresponds to a change in the entry 01101ξ10 starting with $\xi = 1$, both the entropy density and the excess entropy have only one jump for a value of $1 - 0.03$ (see figure 4). ECA 110 is a complex rule where Universal Turing Machine computation capabilities have been found [16]. ECA 106 has been reported to be a complex rule, but the spatiotemporal maps of figure 5 (down) shows that in rule 106, we do not find the same time persistence of local structures as those found in rule 110. At the intermediate values of ξ, the spatiotemporal maps show a behavior more resembling rule 106, which corroborates the entropic measures result. This type of transition is typical of the second one. At one extreme ($\xi = 0$) rule 106, local characteristic patterns are found in the spatiotemporal maps, as ξ changes these features become smaller ($\xi = 0.03$) up to a value ($\xi = 0.97$) where a qualitative change in behavior is observed. The final rule ($\xi = 1$) exhibit a different dynamics than the original one.
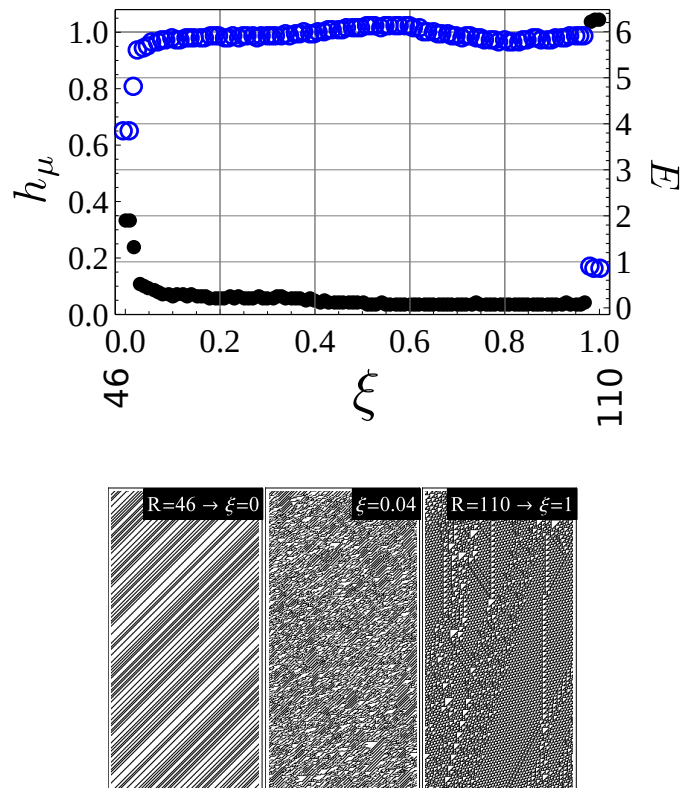

Figure 6. (up) Entropy density (blue) and excess entropy (black) behaviour along the transition 110(01101110) → 46(00101110). This type of transition is characterize by two jump in the entropy density and the excess entropy as the (0ξ101110) entry changes value. Rule 46 is a shift rule where the initial values are shifted to the left one cell at each time step. (down) Spatio-temporal map of both discrete rules and a rule at an intermediate value of ξ.

For rule ECA 110 as we change the six (counting start at zero) entry 0ξ101110 towards rule 46, the third type of behavior is found (see figure 6 (up)). In this case, two jumps in the entropic measures can be observed, resulting in that for intermediate values of ξ, the qualitative behavior of the spatiotemporal maps is different from both extreme discrete rules. ECA 46 is a shift map. It shifts the initial configuration one cell to the left

at each time step, as can be seen in the first spatiotemporal map of figure 6 (down)). For intermediate values of ξ, the spatiotemporal map is different from both discrete ECA rules, as observed in the second spatiotemporal map of figure 6 (down). This intermediate rule exhibits large values of h_μ and small values of excess entropy, pointing to chaotic behavior. A similar transition is found for all entries of the rule 110 except $01101\xi10$ described previously.
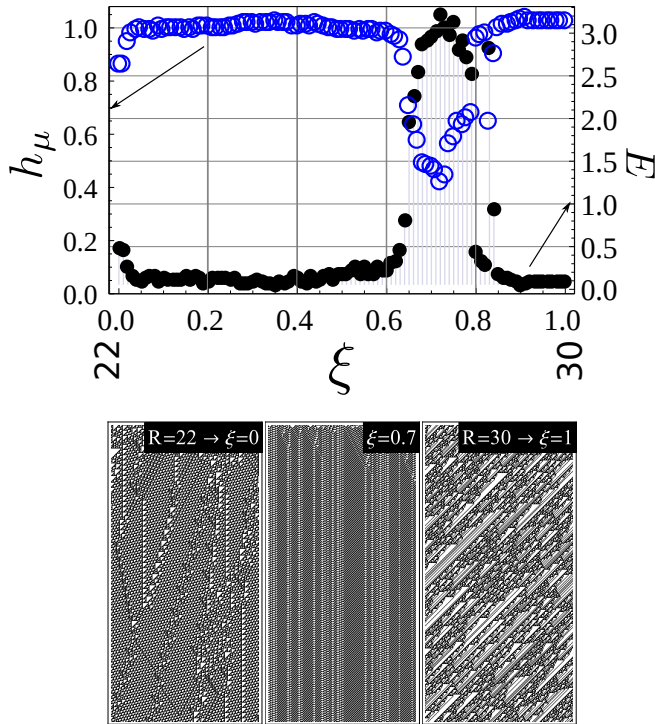

Figure 7. (up) Entropy density (blue) and excess entropy (black) behaviour along the transition $22(00011010) \rightarrow 30(00011110)$. This type of transition is characterized by two jumps in the entropy density and the excess entropy as the $(00011\xi10)$ entry changes value. Rule 22 is an interesting rule, with an initial configuration of only one cell set to one, it develops a fractal structure following the Pascal triangle construction. (down) Both discrete rules give rise to chaotic spatiotemporal maps, at an intermediate value of ξ loss of randomness and increase structuring is observed.

The transition from ECA 22 to ECA 30 is another example of a transition with two clear jumps in the entropy measures but different from the previous example. As figure 7 shows, the discrete rules are spatially chaotic as seen through the entropy density and the excess entropy yet, in the interval of $\xi \in [0.63, 0.8]$ to lower values of entropy density and larger values of excess entropy. h_μ does not decrease to zero, but to an intermediate value slightly above 0.4, while E jumps to a value of 3. The intermediate value of information production and increased information structuring can be observed in the second map of figure 7 (down).

The transition from rule 78 to rule 76 is an example of an irregular transition as measured by the entropic magnitudes (Figure 8 (up)). Rule 76 has binary representation 01001110 and changing the second entry $010011\xi0$ moves towards rule 78 (01001100). After a few steps, both rules are trivial, as can be seen in Figure 8 (down). Rule 76 only differs from the identity rule in the entry of the most significant bit, while rule 78 differs in two entries from the identity rule. Starting from

a random initial configuration rule, 76 does little in terms of ordering, and as a result, entropy density remains high, while almost no structuring is performed and $E = 0$. At a ξ value around 0.05, this dynamics is lost. h_μ jumps to values around 0.15, and excess entropy jumps to values around 3. From there on, both measures fluctuate. Fluctuations in h_μ ranges from 0 to 0.7, while in E from 1.6 to 5. The reader must notice that there is no unique dependency between h_μ and E, the same value of entropy density can result in different values of excess entropy, showing that the different continuous rules are of different natures. From the value $\xi = 0.8$ to 1, the dynamics as measured by h_μ and E settles to values around those found for the rule 78. Rule 78 is able to transform the initial random condition and perform some amount of structuring as both h_μ and E attains intermediate values. Rule 78 is 1-balanced, so erasure of one symbol is not a driving force in the structuring of the initial configuration.
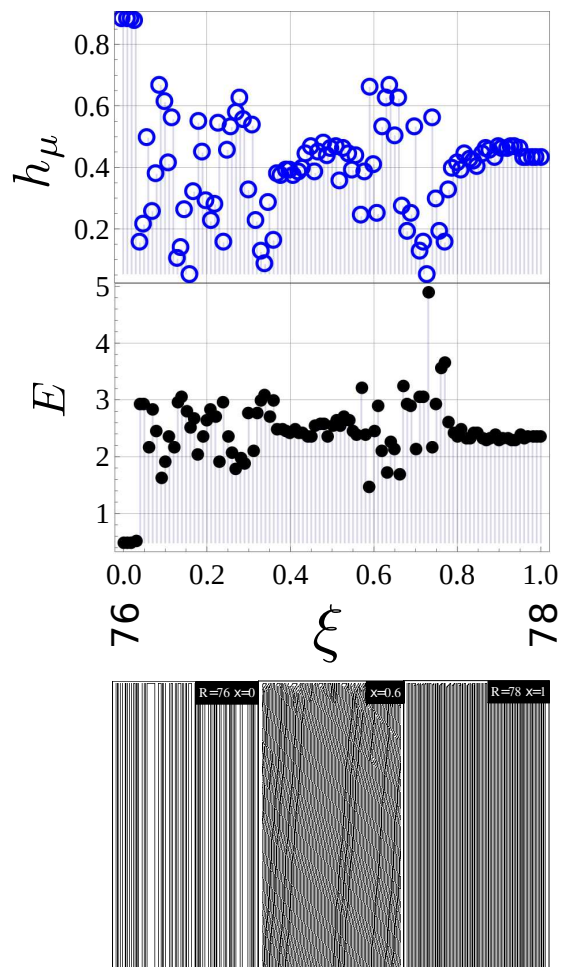

Figure 8. (up) Entropy density (blue) and excess entropy (black) behaviour along the transition $76(01001100) \rightarrow 78(01001110)$. This type of transition is characterize by an irregular behaviour of both the entropy density and the excess entropy as the $(010011\xi0)$ entry changes value. (down) Spatio-temporal map of the discrete rules and an intermediate rule with $\xi = 0.6$. After a transient interval, both discrete rules are rather trivial.

Finally, a different type of transition is shown in figure 9. The transition is from rule $46 \rightarrow 62$, but in figure 9 only the initial region of the transition is shown. The striking feature of this transition is the occurrence of a peak for the excess entropy just before a jump of h_μ towards higher values. At the same point,

d_{LZ} also has a jump. This transition has been described before and claimed to be a fingerprint of enhanced computation at the edge of chaos [14]. The spatiotemporal maps show a shift behaviour for rule 46 (9a), right to the phase transition chaotic behaviour is recognized (9c). At the edge of chaos (9b), the spatiotemporal map is more complex, showing a mixture of shift behavior and the production of features that persist in time and interact between them.
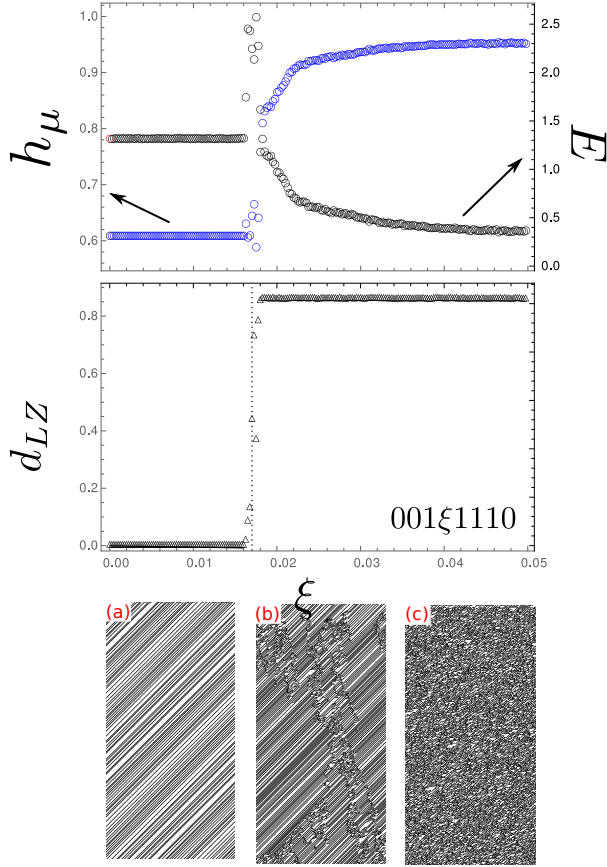

Figure 9. (upper) Entropy density (blue) and excess entropy (black) behavior in a small initial interval of the transition $46 \rightarrow 63$. (middle) The information distance d_{LZ} between two one cell perturbed initial condition after a large number of time steps. A peak in the excess entropy happens just on the verge of a jump in the entropy density towards chaotic behavior. This is further emphasized by the fact that the sensitivity to the initial conditions, as measured by d_{LZ}, has a jump to higher values at the same values where the jump in h_μ can be seen. This behavior is taken as evidence for enhanced computation at the edge of chaos. (lower) (a) corresponds to the spatial-temporal maps at $\xi = 0$; (b) at the $\xi = 0.018$ value where the E attains a maximum and; (c) at $\xi = 0.05$.

A transition with similar feature and yet different in other aspects are that of rule $146 \rightarrow 144$ shown in figure 10. In the interval $\xi \in [0.12, 0.3]$ several transitions occurs. The system at rule 144 has a value of entropy density around 0.57 that drops to zero at $\xi = 0.12$. The excess extropy, which was around 0.2, also drops to zero. At $\xi = 0.2$ h_μ has a jump to 0.85 and increases in a short interval to reach 1 at $\xi = 0.3$. Just before the jump of the entropy density, a very narrow peak in excess entropy can be seen, reaching a value of 4 to drop immediately reaching zero at $\xi = 0.3$ (figure 10left). The spatiotemporal maps (10right) help to understand the transitions. At $\xi = 0.18$ where $h_\mu = 0$, the map shows the occurrence of a triggering effect. Erasure of symbols starts

at some time step rapidly evolving to overtake the whole spatial configuration, $E = 0$ due to the constant nature of the arrangement. At $\xi = 0.22$, where E has a maximum, restructuring of the initial random condition happens at an initial transient stage of a few steps and then a combination of shift map and the emergence of local features with small-time span can be seen which appear random. Finally, at $\xi = 0.3$, a random map shows small, uncorrelated, short-lived features. Although it is clear that the surge of excess entropy is related to a spatiotemporal map with better processing, production, and storage of information, the spatiotemporal map is by no means complex, perhaps pointing to an insufficient improvement of those abilities.
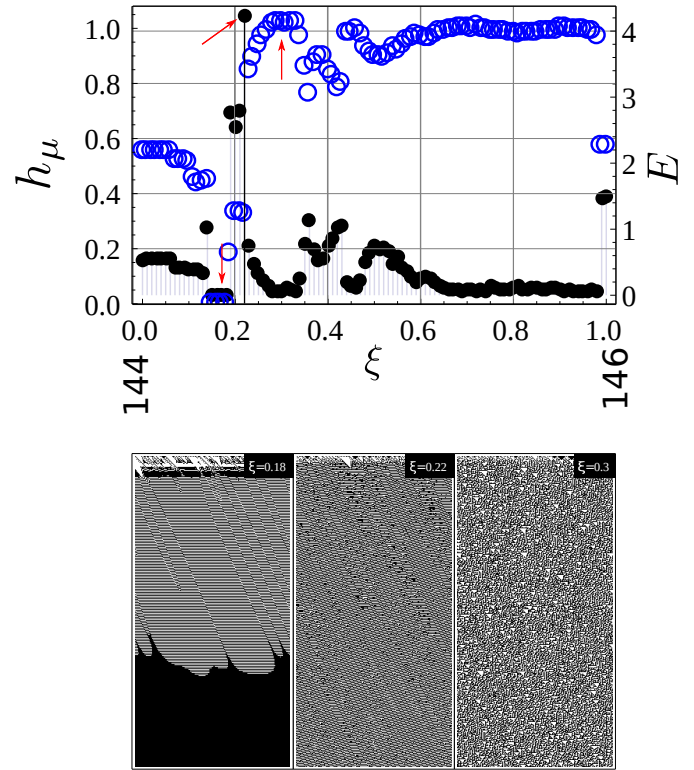

Figure 10. (up) Entropy density (blue) and excess entropy (black) behaviour along the transition $144 \rightarrow 146$. A peak in the excess entropy happens just on the verge of a jump in the entropy density towards chaotic behaviour, before that at $\xi \approx 0.18$ entropy density and excess entropy drops to zero.(down) Spatio-temporal maps of the three points marked with arrow in the right plot. See text for details.

V. CONCLUSION

The results show the richness of transitions that can be found in ECA rules. For those transitions between discrete rules that involve intervals with chaotic behavior ($h_\mu \approx 1$, $E = 0$), memory is necessarily lost in the transition: both discrete ECA rules do not share information in terms of behavior. EOC can happen in a number of transition and indeed has been reported for a number of them, the nature of the EOC can show different variations, but all involve a surge in the excess entropy at the onset of chaos. Our work suggests that if more than two entries in the look-up table are changed simultaneously, unexplored regions can emerge in a two-dimensional phase space. Such simulations have been

performed and will be reported elsewhere. In this regard, what we are witnessing in our results, can be the one-dimensional intercept of such regions, which could explain some of the observed behaviors as a projection of regions from higher dimensions.

REFERENCES

[1] J. P. Crutchfield, Nature **8**, 17 (2012).
[2] S. Wolfram, Theory and applications of cellular automata (World Scientific Press, Singapur, 1986).
[3] J. Kari, Th Comp Science **334**, 3 (2005).
[4] J. P. Crutchfield and K. Young, W. H. Zurek, ed., Complexity, entropy, and the physics of information, 223-269 (Addison Wesley, Redwood City, 1990).
[5] C. G.Langton, Physica D **42**, 12 (1990).
[6] S. A. Kauffman and S. Johnson, C. Langton, G. Taylor, J. D. Farmer and S. Rasmussen, eds., Artificial Life II, 325-368 (Addison Wesley, Redwood City, 1992).
[7] J. P. Crutchfield, P. T. Haber and M. Mitchell, Comput Systems **7**, 89 (1993).
[8] Z. Su, R. W. Rollins and E. R. Hunt, Phys Rev A **40**, 2689 (1989).
[9] R. V. Sole, S. C. Manrubia, B. Luque, J. Delgado and J. Bascompte, Complexity XX, 13 (1996).
[10] N. Bertschinger and T. Natschlager, Neural computation **16**, 1413 (2004).
[11] J. M. Beggs, Phil Trans of the Royal Soc of London A: Math, Phys and Eng Science **366**, 329 (2008).
[12] J. Boedecker, O. Obst, J. T. Lizier, N. M. Mayer and M. Asada, Theory in Bioscience **131**, 205 (2012).
[13] N. H.Packard, J. A. S. Kelso, A. J. Mandell and M. F. Shlesinger, eds., Dynamic patterns in complex systems, 293-301 (World Scientific, Singapore, 1988).
[14] E. Estevez-Rams, D. Estevez-Moya, K. Garcia-Medina and R. Lora-Serrano, Chaos **29**, 043105 (2019).
[15] J. Pedersen, Complex systems **4**, 653 (1990).
[16] S. Wolfram, A new kind of science (Wolfram media Inc., Champaign, Illinois, 2002).
[17] J.-C. Dubacq, B. Durand and E. Formenti, Th Comp Science **259**, 271 (2001).
[18] G. A. Hedlund, Math Systems Theory **3**, 320 (1969).
[19] T. M. Cover and J. A. Thomas, Elements of information theory. Second edition (Wiley Interscience, New Jersey, 2006).
[20] T. Schurmann and P. Grassberg, Chaos **6**, 414 (1999).
[21] A. Lesne, J.L.Blanc and L. Pezard, Phys Rev E **79**, 046208 (2009).
[22] A. Lempel and J. Ziv, IEEE Trans Inf Th IT-22, 75 (1976).
[23] E. Estevez-Rams, R. Lora-Serrano, C. A. J. Nunes and B. Aragón-Fernández, Chaos **25**, 123106 (2015).
[24] P. Grassberger, Int J Theo Phys **25**, 907 (1986).
[25] J. P. Crutchfield and D. Feldman, Chaos **13**, 25 (2003).
[26] O. Melchert and A. K. Hartmann, Phys Rev E **91**, 023306 (2015).
[27] A. N. Kolmogorov, Probl Inf Transm (English Trans) **1**, 1 (1965).
[28] M. Li, X. Chen, X. Li, B. Ma and P. M. B. Vitanyi, IEEE Trans Inf Th **50**, 3250 (2004).